Development of a new CEDAR for kaon identification at the NA62 experiment at CERN

Bethani, A.; Fry, John; Gonnella, Francesco; Goudzovski, Evgueni; Hancock, Jonathan; Henshaw, Jack; Kenworthy, Chandler; Lazzeroni, Cristina; Parkinson, Chris; Romano, Angela; Sanders, Jack; Sergi, Antonino; Shaikhiev, Artur; Tomczak, Adam; NA62 Collaboration

SISSA

Development of a new CEDAR for kaon identification at the NA62 experiment at CERN

View the article online for updates and enhancements.

Development of a new CEDAR for kaon identification at the NA62 experiment at CERN

The NA62 collaboration

E-mail: na62eb@cern.ch

Abstract: The NA62 experiment at CERN utilises a differential Cherenkov counter with achromatic ring focus (CEDAR) for tagging kaons within an unseparated monochromatic beam of charged hadrons. The CEDAR-H detector was developed to minimise the amount of material in the path of the beam by using hydrogen gas as the radiator medium. The detector was shown to satisfy the kaon tagging requirements in a test-beam before installation and commissioning at the experiment. The CEDAR-H performance was measured using NA62 data collected in 2023.

Contents

1 Introduction

The NA62 experiment at CERN [1] is designed to measure the branching fraction of the $K^+ \to \pi^+ \nu \bar{\nu}$ decay, predicted to be $(8.4 \pm 1.0) \times 10^{-11}$ [2], as a stringent test of the Standard Model. First results based on data collected in 2016–2018 have been published [3].

The layout of the NA62 beamline and detector is shown schematically in figure 1. An unseparated secondary hadron beam is produced by directing 400 GeV/c protons extracted from the CERN SPS onto a beryllium target in spills of 4.8 s duration. The nominal particle rate in the beam is 600 MHz, comprising π^+ (70%), protons (23%) and K^+ (6%). The central beam momentum is 75 GeV/c, with a spread of 1% (rms). The beam travels mostly in vacuum from the target, through a fiducial volume that extends between 105 m and 180 m from the target, and ends in a beam dump. The experiment is equipped with a beam spectrometer (GTK) composed of four silicon-pixel detector stations, with the most upstream station located 80 m from the target and the most downstream station (GTK3) located 102 m from the target; a STRAW spectrometer located downstream of the fiducial volume, between 180 and 220 m from the target; and hodoscopes (CHOD) located 238 m from the target. The other principal subdetectors are two Cherenkov counters (KTAG, RICH), a hermetic photon veto (LAV, LKr, IRC, SAC), a hadronic calorimeter (MUV1,2) and a muon system (MUV3). Data from the detectors are collected via a two-stage trigger system, with the first stage implemented in hardware and the latter implemented in software.

Charged kaons are tagged to suppress backgrounds from interactions of beam pions with material on the beamline. Kaon tagging is achieved via the KTAG — a differential Cherenkov counter with achromatic ring focus (CEDAR) [4] connected to a bespoke photon-detection system [5]. The K^+ must be identified with efficiency above 95%, and the kaon-pion separation must be better than 10^4, meaning
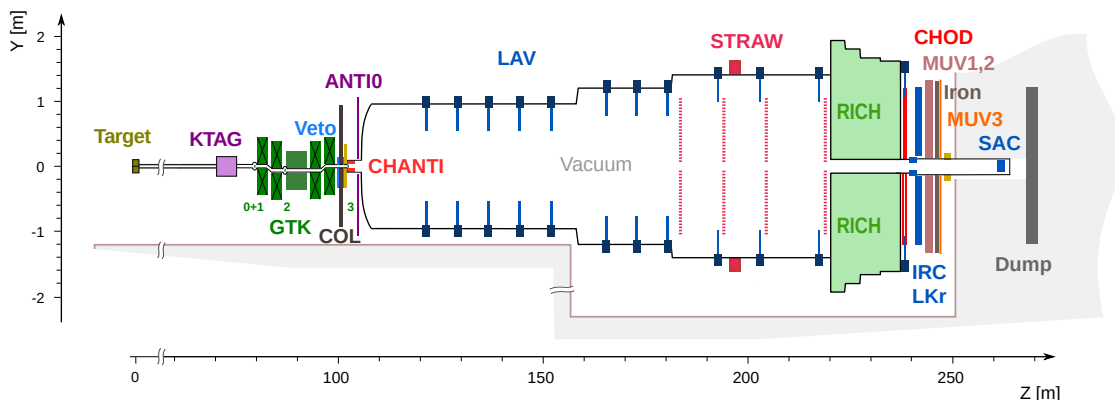
Figure 1. Schematic side view of the NA62 beamline and detector in 2021.

that for each misidentified pion there are more than 10^4 correctly identified kaons. The time resolution must be better than 100 ps to provide a precise time reference for event reconstruction and selection.

The CEDAR was originally developed at CERN with two variants — North (CEDAR-N) and West (CEDAR-W) — adapted for different beam momenta [4]. At NA62, the CEDAR extends from 70 m to 75 m downstream of the target. The CEDAR utilises a gaseous radiator to produce Cherenkov light, and each end of the gas vessel connects to a vacuum beam pipe. Gas in the vessel is isolated from the vacuum in the beam pipe by two aluminium windows of thickness 150 μm and 200 μm. Both the gas and the aluminium windows contribute to the material in the path of the beam.

From the start of NA62 data-taking in 2016, the KTAG used a CEDAR-W filled with nitrogen gas (N_2) at 1.71 bar (in this paper, pressure values refer to absolute pressure). In this configuration, the CEDAR introduces $39 \times 10^{-3} X_0$ of material in the path of the beam, where X_0 is one radiation length. This comprises $35 \times 10^{-3} X_0$ from the N_2 gas and $3.9 \times 10^{-3} X_0$ from the aluminium windows. Multiple scattering of the beam particles introduces an angular divergence of 32 μrad (rms) in both the horizontal and vertical planes, which adds quadratically to the nominal 70 μrad beam divergence at the CEDAR position.

Filling the CEDAR with H_2 at 3.85 bar, as required to achieve a similar Cherenkov angle to N_2 at 1.71 bar, reduces the material in the path of the beam to $7.3 \times 10^{-3} X_0$. This comprises $3.4 \times 10^{-3} X_0$ from the H_2 gas and $3.9 \times 10^{-3} X_0$ from the aluminium windows. In this case, multiple scattering introduces an angular divergence of 13 μrad (rms) in both the horizontal and vertical planes.

Considering the $20 \times 10^{-3} X_0$ contribution of the four GTK stations, replacing the N_2 with H_2 reduces the total material in the path of the beam from $59 \times 10^{-3} X_0$ to $27 \times 10^{-3} X_0$. A full simulation of NA62 implemented with the GEANT4 toolkit [6] shows that the fraction of beam particles interacting inelastically with material upstream of the fiducial volume decreases from 2.1% to 0.9%, in agreement with the above expectation. The simulation also indicates a similar reduction in elastic scattering.

The reduction of scattering in the CEDAR filled with H_2 improves kaon transmission and reduces signal rates in the downstream detectors, and leads to a more efficient selection of $K^+ \to \pi^+ \nu \bar{\nu}$ decays. Furthermore, it is expected to improve the performance of the hardware trigger designed to collect $K^+ \to \pi^+ \nu \bar{\nu}$ decays. In 40% of the events collected via this trigger during 2022, when using the CEDAR-W filled with N_2, the STRAW track closest to the trigger time is consistent with an elastically-
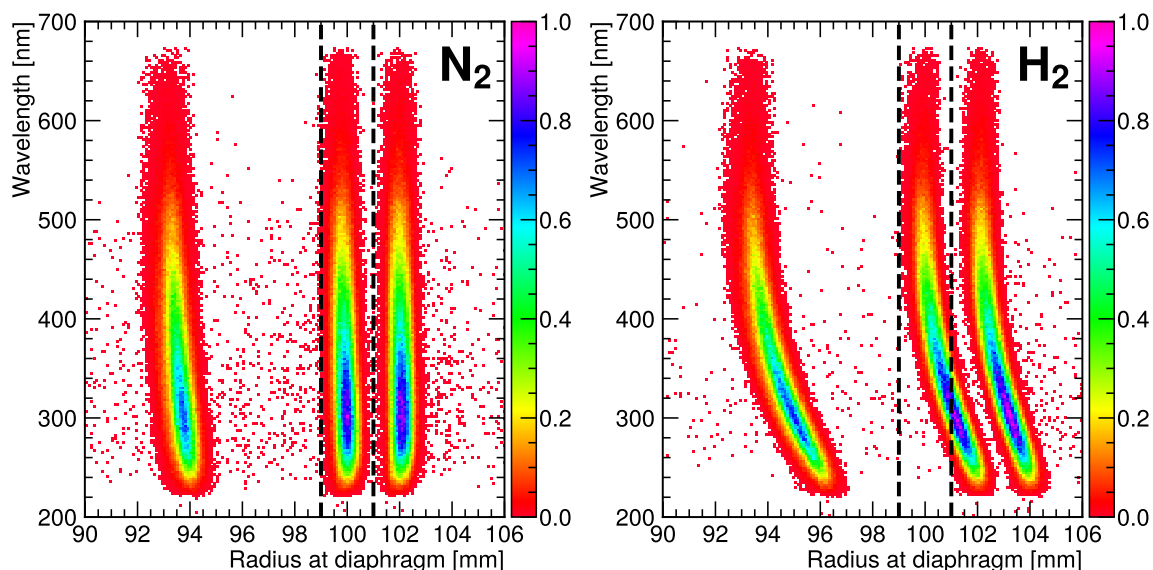
Figure 2. Simulated radial position of Cherenkov photons at the location of the diaphragm in CEDAR-W for proton (lowest radius), kaon and pion (highest radius) beam particles as a function of wavelength with N_2 at 1.71 bar (left panel) and H_2 at 3.67 bar (right panel). The quantum efficiency of the KTAG photomultiplier tubes and the transmittance of the glass filters are imposed. Dashed lines show the extent of a 2.0 mm diaphragm aperture centred at 100 mm.

scattered beam particle originating upstream of GTK3. This suggests that beam particles elastically scattering in CEDAR-W are responsible for a substantial fraction of the hardware trigger rate. The simulation shows that a CEDAR filled with H_2 rather than N_2 reduces the flux of elastically-scattered beam particles passing through detectors downstream of the fiducial volume by 40%, which would reduce the rate of the hardware trigger used to collect $K^+ \rightarrow \pi^+ \nu \bar{\nu}$ decays by 15%. The lower trigger rate will improve the stability of the data acquisition, and will allow looser trigger conditions to be imposed without an overall increase in the trigger rate.

Using H_2 in an existing North or West-type CEDAR does not lead to satisfactory kaon tagging performance, as the chromatic dispersion in H_2 is not corrected by the optical system, and the kaon and pion rings overlap due to their large widths. For the CEDAR-W filled with H_2, a pressure of 3.67 bar optimises the kaon-pion separation. However, 40% of the Cherenkov light is lost as it falls outside of a 2.0 mm diaphragm aperture centred at 100 mm (figure 2) and the detector is unable to satisfy the kaon tagging requirements. As no suitable CEDAR existed, a new detector named CEDAR-H was developed by refitting a North-type CEDAR with optics designed specifically for use with H_2.

2 CEDAR description

Each CEDAR comprises a thermally-insulated gas vessel built in two parts: a 4.5 m long cylinder of 53 cm inner diameter and a vessel cap either 28 cm (CEDAR-N) or 34 cm (CEDAR-W) long attached to the upstream end. The hadron beam passes along the longitudinal axis of the CEDAR.

The CEDAR optical system is contained within the gas vessel, with the optical axis aligned to the longitudinal axis of the CEDAR (figure 3). The light produced in the gas radiator is focused to a ring of mean radius 100 mm at the position of a diaphragm, achieved by the combination of a Mangin
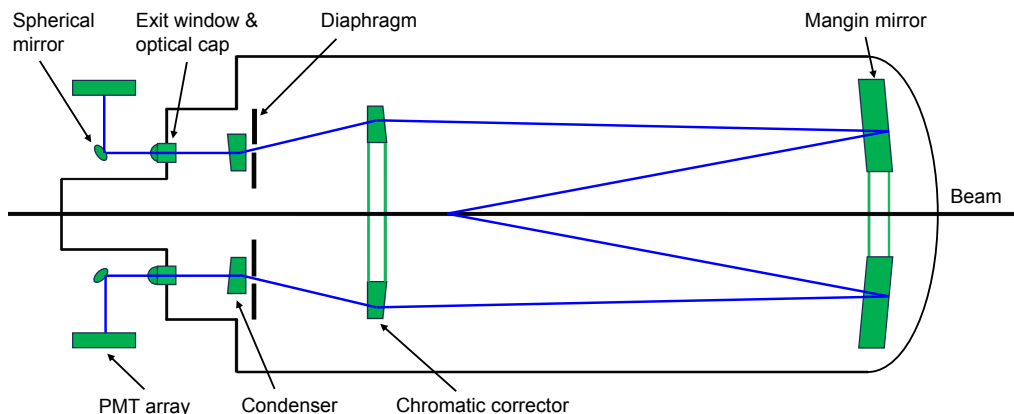
Figure 3. Sketch of the KTAG optical system (not to scale), highlighting the optical elements (green areas) and the path of Cherenkov light (blue lines).

mirror [7] and a chromatic corrector lens. The Mangin mirror is designed to reduce geometrical aberrations; it comprises a lens with two spherical surfaces with the downstream surface cemented onto a concave mirror. The chromatic corrector is a plano-convex lens whose function is to compensate chromatic dispersion in the gas and lenses. Both the Mangin mirror and chromatic corrector have a central hole for the hadron beam to pass through.

The diaphragm is an annular aperture centred at 100 mm, whose width can be varied from zero to 20 mm. Cherenkov light that passes through the aperture traverses condenser lenses that direct the light out of the gas vessel via eight quartz exit windows. The exit windows are equally spaced in azimuth, encircling the beam pipe on the upstream end of the CEDAR. Filters made of glass are glued to the outside of the exit windows to attenuate light with wavelength below 240 nm.

In the original CEDAR design, light exiting the CEDAR is detected by eight ET 9820QB photomultiplier tubes (PMTs), with one PMT positioned on the outside of each exit window. These PMTs cannot sustain the particle rate at NA62, so a new photon-detection system was developed [5]. In the NA62 setup (figure 3) the light travels through optical caps — a set of lenses attached to the outer frames of the exit windows — and passes into the KTAG photon-detection system, which is housed in an enclosure. The light reaches eight spherical mirrors and is reflected through 90 degrees to eight KTAG sectors. Each sector is a PMT array $16 \times 20 \, \text{cm}^2$ in size equipped with 48 Hamamatsu PMTs, 32 of type R9880U-110 and 16 of type R7400U-03, which are sensitive to light with wavelength above 230 nm. Spherical mirrors are used to broaden the light spot and reduce the intensity of photons on the PMTs.

The radius of the Cherenkov rings produced by beam particles passing through the CEDAR depends on the density of gas inside the vessel; increasing the gas pressure increases the refractive index, hence yields larger Cherenkov rings. As such, the gas pressure can be set to obtain a kaon ring of radius 100 mm, matching the central radius of the diaphragm aperture. For gas at a temperature of 293 K and beam particles with momenta of 75 GeV/c, the appropriate gas pressure is 1.71 bar for CEDAR-W and 3.85 bar for CEDAR-H, with a change of 0.34% in these values for each 1 K of temperature difference. Once the operating pressure has been established, the CEDAR is designed to operate with a fixed amount of gas and is therefore insensitive to gradual changes in temperature of the environment. The CEDAR is nevertheless enclosed by thermal insulation to avoid any rapid change in ambient temperature causing differences in the refractive index of the gas at different places within the gas vessel [4].

With the pressure set to obtain a kaon ring of radius 100 mm, the pion and proton rings have radii 102 mm and 94 mm, respectively. Any diaphragm aperture less than 2.5 mm is therefore sufficient to separate the kaon ring from the pion and proton rings. However, beam particles travelling at an angle of 100 μrad with respect to the CEDAR optical axis will produce a Cherenkov ring shifted by 0.5 mm at the diaphragm. Thus, to ensure that the Cherenkov rings are centred on the diaphragm, the beam divergence must be below 100 μrad, and the CEDAR must be parallel to the beam within 100 μrad. The CEDAR is fixed at the upstream end, and can be rotated parallel to the beam via motorised stages situated at its downstream end that can move by ±5 mm horizontally and vertically. Positional offsets of the beam have no effect due to the spherical surface of the Mangin mirror.

3 CEDAR-H development

A CEDAR-N already available at CERN provided the structure of CEDAR-H. No changes to the diaphragm or the optical support structure were envisaged due to their complexity, fixing the positions and outer radii of the Mangin mirror and chromatic-corrector lens, and the position and central radius of the diaphragm. Given these constraints, initial CEDAR-H optical parameters were determined analytically via a ray tracing procedure that sampled the wavelength spectrum and the point of origin of the Cherenkov light. The problem was reduced to two dimensions by exploiting the cylindrical symmetry of the CEDAR. The radii of curvature of the corrector lens and the two surfaces of the Mangin mirror were varied iteratively to achieve a ring of 100 mm radius at the diaphragm with minimal RMS spread. As the relative effects of spherical aberration and chromatic dispersion vary with the gas pressure, the computation was repeated between 3.7 and 4.1 bar in steps of 0.1 bar at a temperature of 293 K, aiming to obtain the best solution at the lowest pressure.

A complete simulation of the KTAG was then employed to refine the analytical solutions using an iterative procedure to minimise the width of the Cherenkov ring. The simulation was then used to identify modifications to the optical system that maximise the amount of light reaching the PMT arrays: the size of the central hole in the Mangin mirror was reduced with respect to the original CEDAR design, making the reflective surface larger, and the radius of curvature of the spherical mirrors was increased so that the distribution of light matched the size and shape of the PMT arrays. The optimum light propagation through the KTAG was achieved with condenser lenses taken from a CEDAR-W rather than a CEDAR-N. It was not necessary to change the optical caps.

The results of the optimisation showed negligible difference in performance between 3.8 bar and 4.1 bar despite greater production of Cherenkov light at higher pressure, primarily because the light spot better matches the PMT arrays at lower pressure. The lower pressure of 3.8 bar is chosen, motivated by H_2 safety considerations. At this pressure, the chromatic dispersion is sufficiently corrected so that the Gaussian width of the kaon and pion rings is 0.4 mm and the rings do not overlap. However, the proton ring is twice as large and distorted due to chromatic dispersion effects (figure 4).

The identification of a particle in the KTAG is defined by detecting coincident light in multiple sectors. Requiring a coincidence in a larger number of sectors reduces the K^+ identification efficiency, while requiring a coincidence in a smaller number of sectors increases the pion misidentification probability. A 5-fold sector coincidence has been the standard kaon tagging requirement since 2016 [1], and corresponds to light detected in 5 or more sectors. In the CEDAR-H simulation, this requirement leads to K^+ identification efficiency of 99.5% and pion misidentification probability below 10^{-4} for a 2 mm diaphragm aperture. These values exceed the kaon tagging requirements.
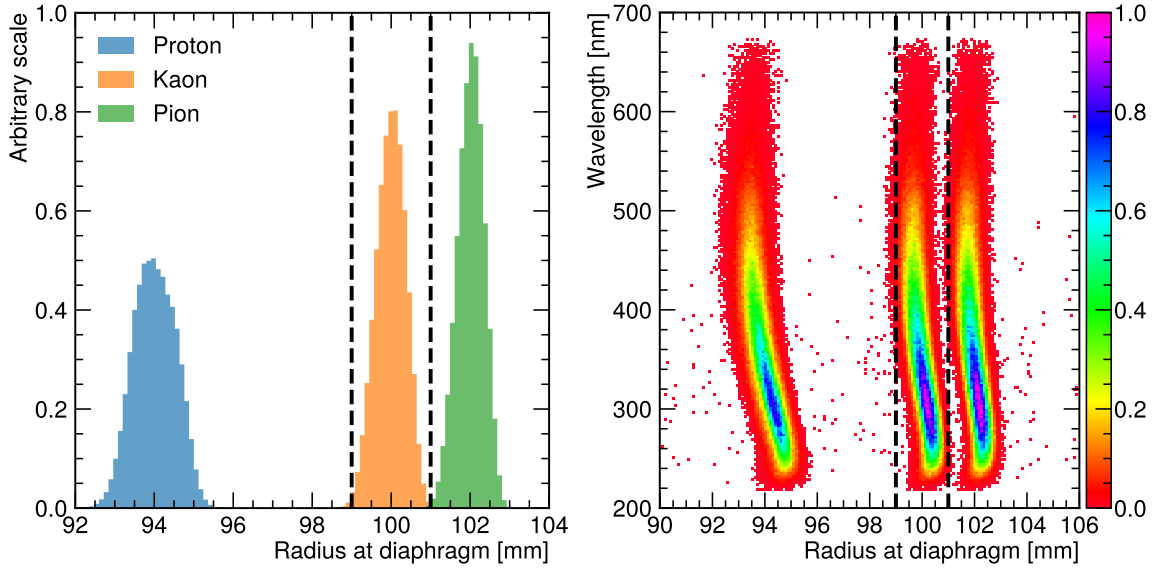
Figure 4. Simulated radial position at the diaphragm of Cherenkov photons for proton, kaon and pion beam particles with CEDAR-H at 3.8 bar (left panel), and as a function of wavelength (right panel). The quantum efficiency of the KTAG photomultipliers and the transmittance of the glass filters are imposed. The three distributions are normalised to the same integral. Dashed lines show the extent of a 2.0 mm diaphragm aperture centred at 100 mm.

Figure 5. CEDAR-H under construction in a clean room at CERN. The photo shows the cylindrical gas vessel (silver-coloured part on the left of the image) and the support structure of the optical system (black part) sitting on a specialised CEDAR workbench (red part). The diaphragm can be seen at the end of the support structure on the right of the image.

The list of CEDAR-H and CEDAR-W mechanical and optical parameters is given in table 1. The CEDAR-H was constructed at CERN in 2022 (figure 5). The Mangin mirror and chromatic corrector were fabricated from high-quality quartz blanks with sub-micron tolerances on their shape.

Table 1. Optical and mechanical parameters of CEDAR-W and CEDAR-H. All values are dimensions in millimetres unless otherwise stated. Positions along the beam axis are quoted with respect to the upstream end of the CEDAR.

CEDAR type		CEDAR-W	CEDAR-H
Nominal gas type		N_2	H_2
Nominal pressure [bar]		1.71	3.80
Gas vessel cylinder	Length	4500	4500
	Inner radius	267	267
Gas vessel cap	Length	339	280
	Inner radius	139	139
Chromatic corrector	Position along the beam axis	1855	1902
	Radius of curvature	1385	1307
	Central thickness	20	20
	Inner radius	75	75
	Outer radius	160	160
Mangin mirror	Position along the beam axis	5353	5362
	Radius of curvature:		
	- refracting surface	6615	8994
	- reflecting surface	8610	9770
	Central thickness	40	40
	Inner radius	50	40
	Outer radius	150	150
Diaphragm	Position along the beam axis	872	911
	Aperture central radius	100	100
Condensers	Position along the beam axis	832	871
	Maximum thickness	10	10
	Radius of curvature	300	300
Quartz windows	Position along the beam axis	472	531
	Thickness	10	10
	Radius	22.5	22.5
	Radial distance to window centre	103	103
Optical caps	Position along the beam axis	450	450
	Maximum thickness	4.24	4.24
	Radius of curvature	114.62	114.62
Spherical mirrors	Position along the beam axis	322	322
	Radius of curvature	51.68	77.52
	Diameter	50	50
	Radial distance to mirror centre	106	106

Figure 6. CEDAR-H in preparation for the test-beam on the H6 beamline at CERN.

A laser-based procedure was used to align the optical components with microradian precision, well within the CEDAR-H operating tolerance. New lenses for the spherical mirrors were coated with 90 nm of aluminium as a reflective layer and 10 nm of SiO_2 as a protective layer. The spherical mirrors were aligned using a laser setup to ensure the Cherenkov light is centred on each PMT array. Millimetre precision was achieved on the light spot positions at the PMT arrays.

4   Test-beam at CERN

The CEDAR-H performance was measured at a test-beam in October 2022 on the H6 beamline at CERN (figure 6). The aims were twofold: to validate the performance of the optical components and their alignment inside the gas vessel, and to measure the K^+ identification efficiency and kaon-pion separation.

Both the NA62 and the H6 hadron beams are derived from interactions of the 400 GeV/c primary proton beam from the CERN SPS with beryllium targets at zero production angle in spills of 4.8 s duration. For the test-beam, the momentum of the H6 hadron beam was set to 75 GeV/c, matching the NA62 beam momentum, and CEDAR-H was placed 440 m downstream of the H6 target, compared to 70 m at NA62. The H6 beam composition at the CEDAR-H position was estimated to be 4% kaons, 25% protons and 71% pions, similar to the NA62 beam. The angular divergence of the H6 beam at the CEDAR-H position was 80 µrad both horizontally and vertically, comparable to the 70 µrad at NA62 and within the operating tolerance. The typical number of particles per spill was 2.8×10^5.

For the test-beam, CEDAR-H was equipped with eight ET 9820QB PMTs, operated at a voltage of 2 kV with a 30 mV discriminator threshold to achieve single-photoelectron sensitivity. A pair of scintillator counters, one upstream and one downstream of CEDAR-H, provided a trigger signal for
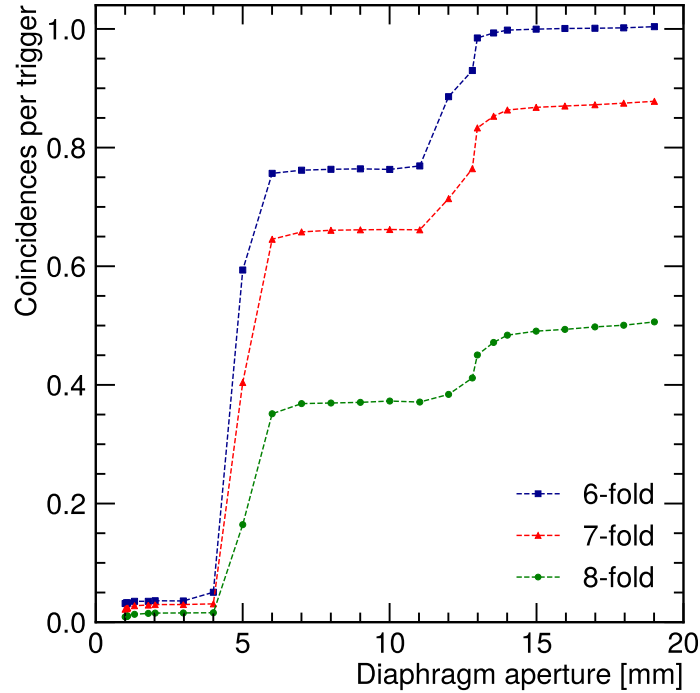
Figure 7. Numbers of 6-fold, 7-fold and 8-fold coincidences per trigger as functions of diaphragm aperture at 3.85 bar, at the H6 test-beam.

each beam particle. The number of triggers, the number of signals in each PMT, and the numbers of 6-fold, 7-fold and 8-fold coincidences in the PMTs were recorded for each spill.

With the H_2 pressure at 4.0 bar and the diaphragm aperture set to 19 mm, Cherenkov light from pions, kaons and protons passed through the diaphragm. In these conditions, the efficiency of each PMT could be measured by the fraction of triggers in which light is detected by the PMT. The mean PMT efficiency was found to be above 98%, and the lowest was 95%.

With the H_2 pressure set to 3.7 bar, the pion ring had a radius of 100 mm, matching the central radius of the diaphragm aperture. With the aperture set to 1.3 mm, only light from the pion passed through the diaphragm. The motorised stages were used to align CEDAR-H parallel to the beam axis, with optimum alignment defined when the PMTs on the top and bottom, and those on the left and right, detected light in the same fraction of triggers. At the end of the alignment procedure, all the PMTs detected light in 70–72% of triggers (consistent with the 71% pion fraction in the beam), which indicated good alignment in both the X and Y directions. The 1.3 mm aperture is the smallest, and therefore most sensitive to the alignment, that was used during the test-beam.

The particle identification efficiency was assessed by measuring the number of 6-fold coincidences per trigger while varying the diaphragm aperture from 0.5 mm to 19.0 mm at 3.85 bar. With the aperture less than 3 mm, the observed 6-fold coincidences were only due to light from the kaon (figure 7). Sharp rises at 4 mm and 11 mm were observed due to light from the pion and proton passing through the diaphragm, respectively. At a diaphragm aperture of 19 mm, a 6-fold coincidence was observed in 99% of triggers.

The CEDAR-H performance with diaphragm apertures ranging from 1.3 mm to 2.3 mm was studied by measuring the number of 6, 7 and 8-fold coincidences per trigger while reducing the
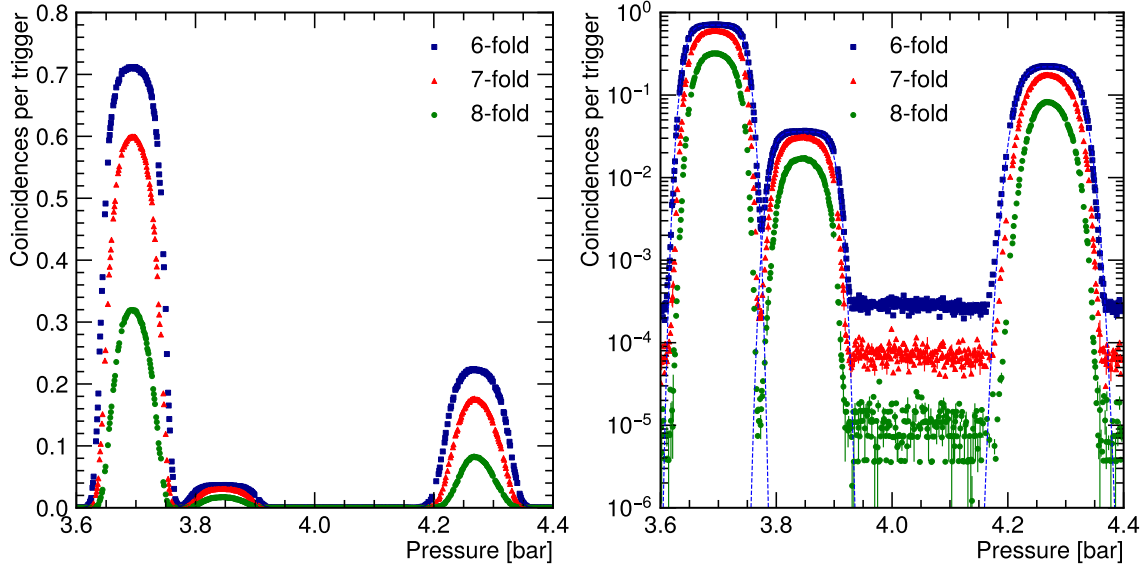
Figure 8. Numbers of 6-fold, 7-fold and 8-fold coincidences per trigger as functions of pressure, at a diaphragm aperture of 1.7 mm, at the H6 test-beam. The three peaks are from the pion (lowest pressure), kaon and proton (highest pressure), shown in linear scale (left panel) and log scale (right panel). The right panel includes fits to the three peaks (dashed lines).

gas pressure from 4.4 to 3.6 bar at each aperture setting. Cherenkov light from the pion, kaon and proton passed through the diaphragm at different pressures, and yielded three distinct peaks, with the centre of the kaon peak at 3.85 bar. The optimal diaphragm aperture was found to be 1.7 mm (figure 8), which maximised the light yield while maintaining an acceptable kaon-pion separation. The light yield was computed from the number of 6, 7 and 8-fold coincidences per trigger measured at 3.85 bar: having defined η_N as the probability of an N-fold coincidence for a given trigger, the mean light yield per beam particle was computed in two ways, as

$$\lambda = \ln\left[1 + \frac{8}{\eta_7/\eta_8 - 1}\right]$$

and

$$\lambda = \ln\left[1 + \frac{14}{\sqrt{4 - 7(1 - \eta_6/\eta_8)} - 2}\right],$$

where the two versions were used to cross-check the result. The above expressions were obtained using binomial statistics and the Poisson distribution of the number of photoelectrons detected in a single sector [4]. The mean light yield per beam particle was found to be 19.1 photoelectrons, with the two equations giving consistent results. The kaon-pion separation was determined to be greater than 10^4 by fitting the observed distribution of the fraction of 6-fold coincidences per trigger as a function of pressure in the region of the pion peak, and extrapolating the fitted function to the centre of the kaon peak. The observed fractions of pions and kaons in the beam, 71% and 4% respectively, were in good agreement with the expected beam composition.

5 CEDAR-H installation at NA62

CEDAR-H was installed on the NA62 beamline with the KTAG photon-detection system attached in March 2023 (figure 9). Several modifications were made to the setup to fulfil the safety requirements imposed by the use of H_2 in the experimental hall, as the CEDAR is not leak-tight and hydrogen gas is flammable when mixed with air in volume concentrations between 4% and 75%.

The volume surrounding any potential H_2 leak is designated as an explosive atmosphere (ATEX) zone 2. To avoid sources of ignition, new temperature sensors with suitable certification for use in an explosive atmosphere are used. There are no electrical connectors in the ATEX zones, and all metal parts in the CEDAR-H area are grounded. Any hydrogen that leaks into confined spaces, such as the KTAG photon-detection system enclosure, is diluted and removed by a flow of nitrogen. Special chimneys have been added to the upstream end of CEDAR-H to avoid accumulation of hydrogen leaking from the gas connections. A safety interlock protects the experiment in case of a hydrogen leak, identified in the gas control system via an unexpected change in the gas pressure over a defined time period. The alarm settings are defined by the sensitivity and stability of the pressure gauges.

A dedicated flammable-gas detector, comprising a metal hood and a metal pavilion, monitors H_2 levels outside of the CEDAR. The metal hood covers the downstream end of CEDAR-H, guiding any leaking gas to a hydrogen sensor and physically separating the motorised stages from any potential gas leak. The metal pavilion covers the upstream end of CEDAR-H, plus the KTAG photon-detection system and the gas distribution panel, to guide any leaking gas to another sensor. The detector issues warning and alarm signals when the H_2 concentration reaches 0.4% and 0.8%, respectively. In case of an alarm signal, power in the area is cut and the CERN fire and rescue service are automatically informed.

The hydrogen leak rate was evaluated during a 10 day test at 3.85 bar. The leak rate was found to be 0.2 litres per day at standard temperature and pressure, satisfying the safety requirements for operating CEDAR-H given the measured airflow and ventilation in the area.

The rupture of a CEDAR aluminium window would result in an uncontrolled release of H_2 from the gas vessel. A safety valve connected to the CEDAR-H exhaust limits the gas pressure to 5 bar to avoid stressing the aluminium windows. Each window is tested at 7.5 bar before installation. A safety interlock is activated if there is a sudden drop in the gas pressure that indicates one of the aluminium windows has ruptured.

6 CEDAR-H commissioning at NA62

During the CEDAR-H commissioning, the beam intensity was set to 10% of the nominal value, which corresponds to a beam particle rate of 60 MHz. Dedicated periodic triggers were used to collect 3×10^5 events per spill.

In standard operating conditions, the KTAG data acquisition records the time and channel ID of each PMT signal in a 100 ns window defined by the trigger time, with each signal corresponding to a single photoelectron. The signals are reconstructed into kaon candidates using a clustering algorithm. The standard time window for the kaon reconstruction is 2 ns, however the relatively low kaon rate during the commissioning allowed a 4 ns time window to be used. On average, 7×10^4 kaon candidates were reconstructed in the data collected in each spill.

Figure 9. CEDAR-H (left panel) and KTAG photon-detection system (right panel) during installation in the experimental hall. In the left panel, the downstream end of CEDAR-H is on the left, and the black enclosure of the KTAG photon-detection system is on the right. In the right panel, the upstream-side of the enclosure is removed, revealing the eight sectors within.

As the KTAG data acquisition records each photoelectron individually, the definition of the light yield and the kaon tagging requirement differ from those used during the test beam. The light yield is defined as the mean number of photoelectrons assigned to the kaon candidates. The kaon tagging requires that signals are observed in at least five sectors, as discussed in section 3.

A coarse angular alignment of CEDAR-H to the beam is performed with the H_2 pressure set to the proton peak (4.3 bar) and the diaphragm aperture set to 6 mm. This stage of the alignment is made by balancing the number of signals in the sectors at the top, bottom, left, and right. The final alignment is performed by maximising the light yield at the pressure of the kaon peak (3.88 bar) and a diaphragm aperture of 1 mm. The optimum alignment yields an average of 21.7 photoelectrons per kaon candidate with the 4 ns time window. Changing the alignment in either the vertical or horizontal plane by one increment, corresponding to 7 µrad, reduces the number of photoelectrons per kaon candidate by 0.02, showing that the performance is insensitive to small changes in alignment. The light yield is 15% larger when using the KTAG PMT arrays instead of the eight PMTs used in the test beam, as expected from the simulation.

With the pressure set to the centre of the kaon peak, the optimum aperture is determined by measuring the number of kaon candidates with 5-fold sector coincidences, normalised to the measured beam intensity, at aperture settings ranging from zero to 6 mm (figure 10). The optimum setting is 1.8 mm, chosen as the smallest value that collects all the light from the kaon.

With the diaphragm aperture set to 1.8 mm, the numbers of 5, 6, 7, and 8-fold coincidences are measured while reducing the pressure from 4.4 to 3.6 bar (figure 11). The centre of the kaon peak is found at 3.88 bar, and differs from the test-beam value (3.85 bar) due to 2 K higher gas temperature during the commissioning at NA62. The kaon-pion separation is measured to be better than 10^4 by fitting the distribution of 5-fold sector coincidences as a function of pressure, as described in section 4.
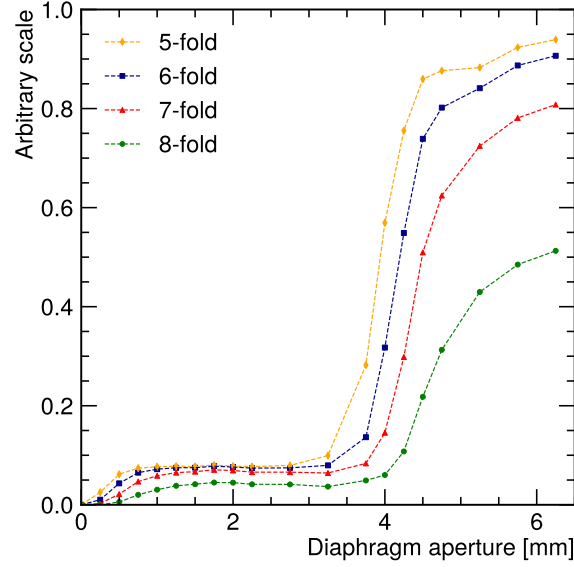
Figure 10. Numbers of reconstructed beam particles with 5-fold, 6-fold, 7-fold and 8-fold sector coincidences per beam particle (normalised arbitrarily), as a function of diaphragm aperture at 3.88 bar, measured using data collected with periodic triggers.
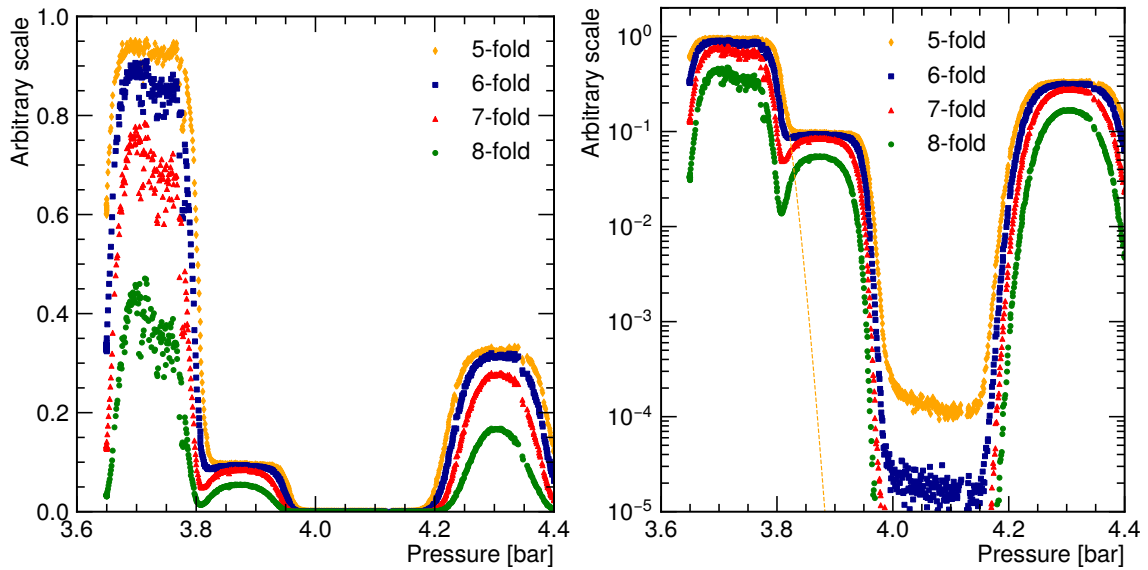
Figure 11. Numbers of reconstructed beam particles with 5-fold, 6-fold, 7-fold and 8-fold sector coincidences in linear scale (left panel) and log scale (right panel). The data were collected with a periodic trigger and a diaphragm aperture of 1.8 mm, and are normalised to the measured beam intensity. The three peaks correspond to the pion (lowest pressure), kaon and proton (highest pressure). The pion peak is distorted due to limitations of the KTAG data acquisition. The right panel includes a fit to the right side of the pion peak (dashed line).

7 CEDAR-H performance at NA62

The CEDAR-H performance in standard NA62 operating conditions is assessed using data collected in 2023, and is compared to that of CEDAR-W using data collected in 2022. A sample of charged kaons
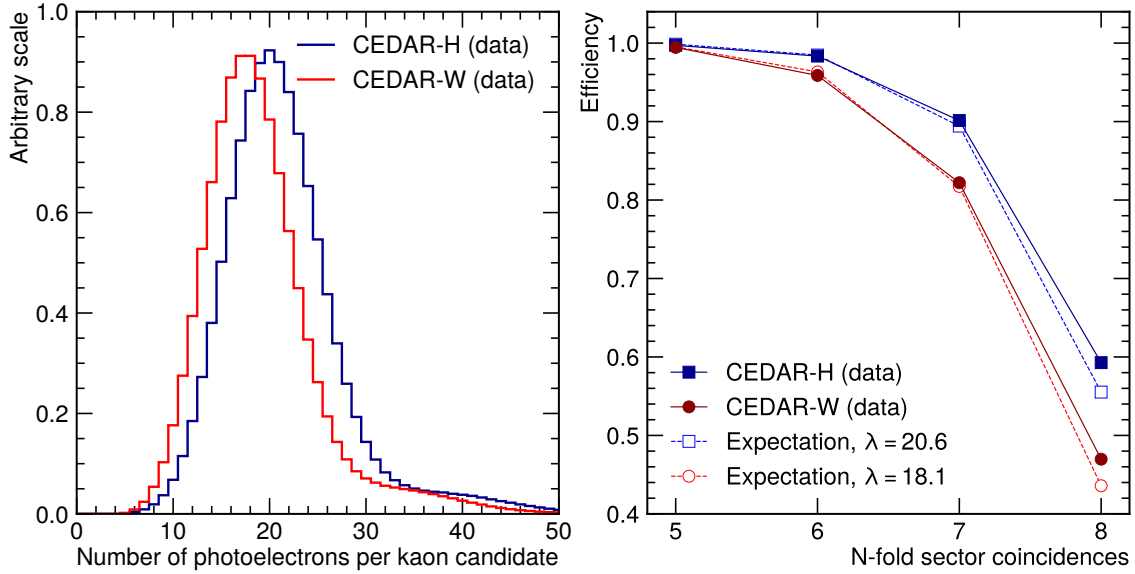
Figure 12. Left: number of photoelectrons per kaon candidate for CEDAR-W and CEDAR-H in the data, reconstructed with a 2 ns time window and normalised to the same integral. Right: K^+ identification efficiency for CEDAR-W and CEDAR-H as a function of N-fold sector coincidences, with analytical expectations for the efficiency given the Poisson mean numbers of photoelectrons of 20.6 and 18.1 from fits to the distributions in the left panel.

is obtained by selecting $K^+ \to \pi^+\pi^+\pi^-$ decays fully reconstructed in the STRAW spectrometer. The decay time is measured with a precision of 200 ps using the information from the CHOD hodoscopes, and kaon candidates are reconstructed in the KTAG data using the standard 2 ns time window.

The light yield and time resolution are measured using kaon candidates with signals in at least 5 sectors and thus satisfy the standard kaon tagging requirement. The light yield is extracted by fitting a Poisson distribution to the observed number of photoelectrons per kaon candidate between 4 and 24, because a tail towards larger numbers of photoelectrons is observed in the data due to the reconstruction of two coincident K^+ as a single kaon candidate (figure 12, left). The light yield achieved with CEDAR-H is 20.6 photoelectrons per kaon candidate, an improvement over 18.1 photoelectrons achieved in 2022 with CEDAR-W. The CEDAR-H time resolution is computed to be 66 ps (compared to 71 ps for CEDAR-W) based on the number of photoelectrons per kaon candidate and the nominal KTAG PMT single-photoelectron time resolution of 300 ps [1].

The K^+ identification efficiency is measured based on the reconstruction of a kaon candidate within 2 ns of the $K^+ \to \pi^+\pi^+\pi^-$ decay time that satisfies the tagging requirement. The K^+ identification efficiency based on 5-fold coincidences is found to be 99.7%, compared to 99.5% for CEDAR-W. The measured efficiency of the two detectors is compared to analytical expectations based on the observed light yield for each detector in figure 12, right. The analytical expectation is computed assuming an ideal detector and a uniform distribution of photoelectrons over the 384 PMTs. The measured efficiency for 8-fold coincidences is higher than the analytical expectation due to the kaon candidates reconstructed from multiple coincident K^+.

Reduction of the elastic scattering of beam particles in CEDAR-H compared to CEDAR-W is investigated by selecting tracks reconstructed in the STRAW spectrometer with a momentum of

75 GeV/c that originate upstream of GTK3. These tracks are selected in data collected via the same minimum-bias hardware trigger in both 2023 and 2022. By normalising to the number of $K^+ \to \pi^+\pi^0$ decays in each data sample, a 30% reduction of elastically scattered beam particles originating upstream of GTK3 is observed with CEDAR-H with respect to CEDAR-W, in agreement with simulation. The corresponding reduction of the trigger rate allowed looser trigger criteria to be imposed in 2023.

8 Summary

A kaon tagger for the NA62 experiment has been developed that minimises the amount of material in the path of the beam. This was accomplished using a North-type CEDAR filled with H_2 and equipped with a specialised optical system designed using a full simulation of the KTAG. The detector performance was validated at a test-beam before installation at the experiment. Several measures were taken to fulfil safety requirements imposed by the use of H_2. After the detector was commissioned, data collected in standard operating conditions show that the kaon-pion separation exceeds 10^4, the time resolution is 66 ps, and the K^+ identification efficiency is 99.7%. Each of these values exceeds the kaon tagging requirements.

References

[1] NA62 collaboration, *The beam and detector of the NA62 experiment at CERN*, 2017 *JINST* **12** P05025 [arXiv:1703.08501].

[2] A.J. Buras, D. Buttazzo, J. Girrbach-Noe and R. Knegjens, $K^+ \rightarrow \pi^+ \nu \overline{\nu}$ and $K_L \rightarrow \pi^0 \nu \overline{\nu}$ in the Standard Model: status and perspectives, *JHEP* **11** (2015) 033 [arXiv:1503.02693].

[3] NA62 collaboration, *Measurement of the very rare $K^+ \rightarrow \pi^+ \nu \overline{\nu}$ decay*, *JHEP* **06** (2021) 093 [arXiv:2103.15389].

[4] C. Bovet et al., *The Cedar Counters for Particle Identification in the SPS Secondary Beams: A Description and an Operation Manual*, Tech. Rep. CERN-82-13, CERN, Geneva, Switzerland (1982) [DOI:10.5170/CERN-1982-013].

[5] E. Goudzovski et al., *Development of the kaon tagging system for the NA62 experiment at CERN*, *Nucl. Instrum. Meth. A* **801** (2015) 86 [arXiv:1509.03773].

[6] GEANT4 collaboration, *GEANT4 — a simulation toolkit*, *Nucl. Instrum. Meth. A* **506** (2003) 250.

[7] M.J. Riedl, *The Mangin mirror and its primary aberrations*, *Appl. Opt.* **13** (1974) 1690.

The NA62 collaboration

Université Catholique de Louvain, Louvain-La-Neuve, Belgium
A. Bethani [ID], E. Cortina Gil [ID], J. Jerhot [ID][1], N. Lurkin [ID]

TRIUMF, Vancouver, British Columbia, Canada
T. Numao [ID], B. Velghe [ID], V.W.S. Wong [ID]

University of British Columbia, Vancouver, British Columbia, Canada
D. Bryman [ID][2]

Charles University, Prague, Czech Republic
Z. Hives [ID], T. Husek [ID][3], K. Kampf [ID], M. Koval [ID]

Aix Marseille University, CNRS/IN2P3, CPPM, Marseille, France
B. De Martino [ID], M. Perrin-Terrin [ID]

Max-Planck-Institut für Physik (Werner-Heisenberg-Institut), Garching, Germany
B. Döbrich [ID], S. Lezki [ID], J. Schubert [ID]

Institut für Physik and PRISMA Cluster of Excellence, Universität Mainz, Mainz, Germany
A. T. Akmete [ID], R. Aliberti [ID][4], L. Di Lella [ID], N. Doble [ID], L. Peruzzo [ID], S. Schuchmann [ID], H. Wahl [ID],
R. Wanke [ID]

Dipartimento di Fisica e Scienze della Terra dell'Università e INFN, Sezione di Ferrara, Ferrara, Italy
P. Dalpiaz, I. Neri [ID], F. Petrucci [ID], M. Soldani [ID]

INFN, Sezione di Ferrara, Ferrara, Italy
L. Bandiera [ID], A. Cotta Ramusino [ID], A. Gianoli [ID], M. Romagnoni [ID], A. Sytov [ID]

Dipartimento di Fisica e Astronomia dell'Università e INFN, Sezione di Firenze, Sesto Fiorentino, Italy
M. Lenti [ID], P. Lo Chiatto [ID], I. Panichi [ID], G. Ruggiero [ID]

INFN, Sezione di Firenze, Sesto Fiorentino, Italy
A. Bizzeti [ID][5], F. Bucci [ID]

Laboratori Nazionali di Frascati, Frascati, Italy
A. Antonelli [ID], V. Kozhuharov [ID][6], G. Lanfranchi [ID], S. Martellotti [ID], M. Moulson [ID], T. Spadaro [ID], G. Tinti [ID]

Dipartimento di Fisica "Ettore Pancini" e INFN, Sezione di Napoli, Napoli, Italy
F. Ambrosino [ID], M. D'Errico [ID], R. Fiorenza [ID][7], R. Giordano [ID], P. Massarotti [ID], M. Mirra [ID],
M. Napolitano [ID], I. Rosa [ID], G. Saracino [ID]

Dipartimento di Fisica e Geologia dell'Università e INFN, Sezione di Perugia, Perugia, Italy
G. Anzivino [ID]

INFN, Sezione di Perugia, Perugia, Italy

P. Cenci ⓘ, V. Duk ⓘ, R. Lollini ⓘ, P. Lubrano ⓘ, M. Pepe ⓘ, M. Piccini ⓘ

Dipartimento di Fisica dell'Università e INFN, Sezione di Pisa, Pisa, Italy

F. Costantini ⓘ, M. Giorgi ⓘ, S. Giudici ⓘ, G. Lamanna ⓘ, E. Lari ⓘ, E. Pedreschi ⓘ, J. Pinzino ⓘ, M. Sozzi ⓘ

INFN, Sezione di Pisa, Pisa, Italy

R. Fantechi ⓘ, F. Spinella ⓘ

Scuola Normale Superiore e INFN, Sezione di Pisa, Pisa, Italy

I. Mannelli ⓘ

Dipartimento di Fisica, Sapienza Università di Roma e INFN, Sezione di Roma I, Roma, Italy

M. Raggi ⓘ

INFN, Sezione di Roma I, Roma, Italy

A. Biagioni ⓘ, P. Cretaro ⓘ, O. Frezza ⓘ, A. Lonardo ⓘ, M. Turisini ⓘ, P. Vicini ⓘ

INFN, Sezione di Roma Tor Vergata, Roma, Italy

R. Ammendola ⓘ, V. Bonaiuto ⓘ[8], A. Fucci, A. Salamon ⓘ, F. Sargeni ⓘ[9]

Dipartimento di Fisica dell'Università e INFN, Sezione di Torino, Torino, Italy

R. Arcidiacono ⓘ[10], B. Bloch-Devaux ⓘ, E. Menichetti ⓘ, E. Migliore ⓘ

INFN, Sezione di Torino, Torino, Italy

C. Biino ⓘ[11], A. Filippi ⓘ, F. Marchetto ⓘ, D. Soldi ⓘ

Instituto de Física, Universidad Autónoma de San Luis Potosí, San Luis Potosí, Mexico

A. Briano Olvera ⓘ, J. Engelfried ⓘ, N. Estrada-Tristan ⓘ[12], R. Piandani ⓘ, M.A. Reyes Santos ⓘ[12], K.A. Rodriguez Rivera ⓘ

Horia Hulubei National Institute for R&D in Physics and Nuclear Engineering, Bucharest-Magurele, Romania

P. Boboc ⓘ, A.M. Bragadireanu, S.A. Ghinescu ⓘ, O.E. Hutanu

Faculty of Mathematics, Physics and Informatics, Comenius University, Bratislava, Slovakia

T. Blazek ⓘ, V. Cerny ⓘ, R. Volpe ⓘ[13]

CERN, European Organization for Nuclear Research, Geneva, Switzerland

J. Bernhard ⓘ, L. Bician ⓘ[14], M. Boretto ⓘ, E. Bravin ⓘ, F. Brizioli ⓘ[15], A. Ceccucci ⓘ, M. Ceoletta ⓘ, M. Corvino ⓘ, H. Danielsson ⓘ, F. Duval, L. Federici ⓘ, Y. Fiammingo ⓘ, E. Gamberini ⓘ, A. Goncalves Martins De Oliveira, R. Guida ⓘ, E.B. Holzer ⓘ, B. Jenninger, Z. Kucerova ⓘ, A. Lafuente Mazuecos ⓘ, G. Lehmann Miotto ⓘ, P. Lichard ⓘ, K. Massri ⓘ, E. Minucci ⓘ[16], M. Noy, G. Rigoletti ⓘ, V. Ryjov, T. Schneider ⓘ, J. Swallow ⓘ[17], P. Wertelaers ⓘ, M. Zamkovsky ⓘ

Ecole Polytechnique Fédérale Lausanne, Lausanne, Switzerland

X. Chang ⓘ, A. Kleimenova ⓘ, R. Marchevski ⓘ

School of Physics and Astronomy, University of Birmingham, Birmingham, United Kingdom

J.R. Fry ⓘ, F. Gonnella ⓘ, E. Goudzovski ⓘ, J. Hancock ⓘ, J. Henshaw ⓘ, C. Kenworthy ⓘ, C. Lazzeroni ⓘ, C. Parkinson ⓘ*, A. Romano ⓘ, J. Sanders ⓘ*, A. Sergi ⓘ[18], A. Shaikhiev ⓘ[19], A. Tomczak ⓘ

School of Physics, University of Bristol, Bristol, United Kingdom

H. Heath ⓘ

School of Physics and Astronomy, University of Glasgow, Glasgow, United Kingdom

D. Britton ⓘ, A. Norton ⓘ, D. Protopopescu ⓘ

Physics Department, University of Lancaster, Lancaster, United Kingdom

J.B. Dainton, L. Gatignon ⓘ, R.W.L. Jones ⓘ

Physics and Astronomy Department, George Mason University, Fairfax, Virginia, U.S.A.

P. Cooper, D. Coward ⓘ[20], P. Rubin ⓘ

Authors affiliated with an Institute or an international laboratory covered by a cooperation agreement with CERN

A. Baeva, D. Baigarashev ⓘ[21], D. Emelyanov, T. Enik ⓘ, V. Falaleev ⓘ[13], S. Fedotov, K. Gorshanov ⓘ, E. Gushchin ⓘ, V. Kekelidze ⓘ, D. Kereibay, S. Kholodenko ⓘ[22], A. Khotyantsev, A. Korotkova, Y. Kudenko ⓘ, V. Kurochka, V. Kurshetsov ⓘ, L. Litov ⓘ[6], D. Madigozhin ⓘ, A. Mefodev, M. Misheva[23], N. Molokanova, V. Obraztsov ⓘ, A. Okhotnikov ⓘ, I. Polenkevich, Yu. Potrebenikov ⓘ, A. Sadovskiy ⓘ, S. Shkarovskiy, V. Sugonyaev ⓘ, O. Yushchenko ⓘ

* *Corresponding authors: C. Parkinson, J. Sanders, email: chris.parkinson@cern.ch, jack.sanders@cern.ch*

[1] *Present address: Max-Planck-Institut für Physik (Werner-Heisenberg-Institut), Garching, D-85748, Germany*

[2] *Also at TRIUMF, Vancouver, British Columbia, V6T 2A3, Canada*

[3] *Also at School of Physics and Astronomy, University of Birmingham, Birmingham, B15 2TT, U.K.*

[4] *Present address: Institut für Kernphysik and Helmholtz Institute Mainz, Universität Mainz, Mainz, D-55099, Germany*

[5] *Also at Dipartimento di Scienze Fisiche, Informatiche e Matematiche, Università di Modena e Reggio Emilia, I-41125 Modena, Italy*

[6] *Also at Faculty of Physics, University of Sofia, BG-1164 Sofia, Bulgaria*

[7] *Present address: Scuola Superiore Meridionale e INFN, Sezione di Napoli, I-80138 Napoli, Italy*

[8] *Also at Department of Industrial Engineering, University of Roma Tor Vergata, I-00173 Roma, Italy*

[9] *Also at Department of Electronic Engineering, University of Roma Tor Vergata, I-00173 Roma, Italy*

[10] *Also at Università degli Studi del Piemonte Orientale, I-13100 Vercelli, Italy*

[11] *Also at Gran Sasso Science Institute, I-67100 L'Aquila, Italy*

[12] *Also at Universidad de Guanajuato, 36000 Guanajuato, Mexico*

[13] *Present address: INFN, Sezione di Perugia, I-06100 Perugia, Italy*

[14] *Present address: Charles University, 116 36 Prague 1, Czech Republic*

[15] *Also at INFN, Sezione di Perugia, I-06100 Perugia, Italy*

[16] *Present address: Syracuse University, Syracuse, NY 13244, U.S.A.*

[17] *Present address: Laboratori Nazionali di Frascati, I-00044 Frascati, Italy*

[18] *Present address: Dipartimento di Fisica dell'Università e INFN, Sezione di Genova, I-16146 Genova, Italy*

[19] *Present address: Physics Department, University of Lancaster, Lancaster, LA1 4YB, U.K.*

[20] *Also at SLAC National Accelerator Laboratory, Stanford University, Menlo Park, CA 94025, U.S.A.*

[21] *Also at L.N. Gumilyov Eurasian National University, 010000 Nur-Sultan, Kazakhstan*

[22] *Present address: INFN, Sezione di Pisa, I-56100 Pisa, Italy*

[23] *Present address: Institute of Nuclear Research and Nuclear Energy of Bulgarian Academy of Science (INRNE-BAS), BG-1784 Sofia, Bulgaria*